Estimation of Dust Emission from the Western Coastal Plains of Arabian Peninsula

A.E. Anisimov, G.L. Stenchikov

King Abdullah University of Science and Technology, Division of Physical Sciences and Engineering, Thuwal, Saudi Arabia

Introduction

Motivation

- The Red Sea, bordered the Sahara and Arabian deserts with little or no river discharge and flash floods from land, is highly oligotrophic, especially in the northern part, hardly attainable by the nutrients coming from the Indian Ocean. The impact of dust deposition on nutrient balance of semi-enclosed Red Sea may be significant;
- Dust storms in the western Arabian Peninsula substantially affect densely-populated metropolitan areas of Makkah, Madinah and Jeddah;
- Satellite images and ground observations show that there is a zone of increased dust activity in the western part of Arabian Peninsula This narrow dust generation zone may be important for nutrient balance of the Red Sea, as located in a close proximity to the Sea.

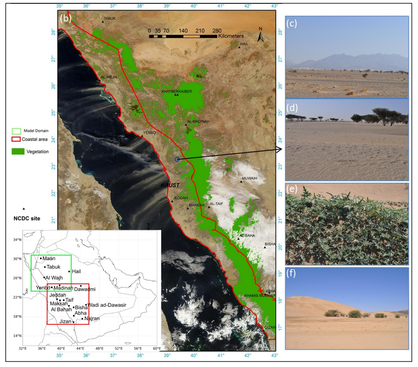

We employ the high-resolution CLM4 **(Community Land Model version-4)** model with the **DEAD (Dust Entrainment and Deposition)** module to calculate dust emissions in the western coast of the Arabian Peninsula. Our principle objectives are:

- to examine the model sensitivity to the type and horizontal resolution of land surface datasets;
- to determine the best model configuration by performing simulations with various types of statistical dust source functions;
- to obtain new, high-resolution estimates of dust emission from the Red Sea Arabian coastal plain.

We use the high-resolution, advanced surface vegetation datasets and demonstrate their benefits. We compare the results with independent weather code and visibility reports from meteorological stations and MERRAero reanalysis. Although these data are indirect with respect to local dust emissions and cannot be applied for accurate model validation, they may provide valuable information and serve as a reference for determining optimal model setup. Finally, we choose the best model configuration and apply it to assess the dust emission from the narrow semi-desert region in the west of Arabian Peninsula. We conduct simulations for three years of **2009 – 2011** with 10-km wind forcing from WRF simulation and present novel estimates of dust emission variability.

Model verification

The results are compared with weather code and visibility reports from **16 meteorological stations** based primarily on sites of domestic and international airports in Saudi Arabia and Jordan.

Temporal variability

Dust event frequency and intensity are validated against station observations:

- Station dust event **frequency** F_d is based on **weather code reports** and defined in a classical way (Shao et al., 2008): $F_d = N_d/N_{tot}$, where N_d is the number of monthly reported dust events, and N_{tot} is the total number of reports (including those when visibility was not reduced below 10000 m and no weather code was reported). To obtain the corresponding time series from model data two constant thresholds of 1 μg/m^2·s and 4 μg/m^2·s were applied.
- Station dust event **intensity** is based on **visibility measurements** and is defined as monthly average visibility reduction when dust event is reported. Corresponding model time series are obtained with the same threshold as frequency.

Model – station monthly Spearman's correlations for:

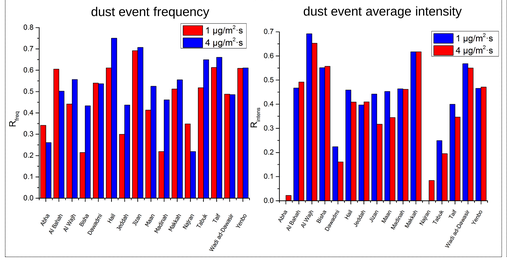

Spatial variability

To analyze the spatial correspondence of model and station data, we sample the hourly visibility time series by dust event reports and calculate the 3-year sampled mean **visibility** for each station. Mean emission rate is calculated for model data by sampling for the same timesteps. In other words, **we compare the mean visibility reduction during intense dust storms with local dust emission rate.**

Having two samples of 3-year mean values, we calculate the correlation coefficient between them. The analysis is performed for three basic experiments and four source functions applied to each of them. The best results were obtained when using **SEVIRI source function**. Depending on model spatial resolution, the significant model skill varied from **0.68 to 0.85**.

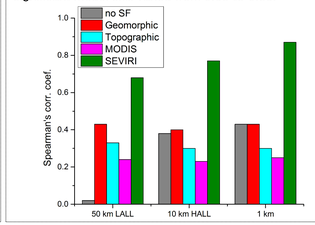

Sensitivity experiments

The original spatial resolution of input datasets

Input data	Parameters affected	CLM4 default	Data used	
		Resolution	Original data resolution	Source
PFT	F_m	0.5° × 0.5°	500m × 500m	MODIS Land Product MYD12
LAI			1km × 1km	MODIS MCD15
SAI			1km × 1km	Calculated from LAI
CLY	α, f_w		1km × 1km	STATSGO-FAO (10km × 10km)
ERD	S	Constant=1	4 types of source functions	

Using high-resolution vegetation dataset results in appreciable increase in total dust generation with comparable contribution from LLAI and LPFT. The changes are not strictly additive and are spatially non-uniform, with the highest differences occurring along the coastal and mountain areas with the substantial vegetation. Total dust emission in LALL is around 10% smaller then in HALL. The separate differences are smaller: 6% (LLAI) and 3% (LPFT). The difference between the HALL and LCLY simulation is not shown, as the changes are very small (less than 1 g/m^2·a) suggesting for weak model sensitivity to the resolution of clay mass fraction dataset.

We extend the sensitivity study by (Shi et al., 2016) for finer scales, examining the sensitivity to the horizontal resolution of plant function type (PFT), leaf area index (LAI), stem area index (SAI), and clay mass fraction (CLY) input surface datasets.

First, we consider the contribution from each of the input surface characteristics separately. We have performed the control experiment with all of the surface data taken at 10 × 10 km resolution (HALL), and four additional simulations. In the LPFT, LLAI, and LCLY experiments, we degrade the spatial resolution of one of the datasets in comparison with HALL to 50 × 50 km.

Spatial resolution of input datasets used in simulations

		Simulation					
		HALL	LALL	SALL	LPFT	LLAI	LCLY
Input data	PFT	10 km	50 km	1 km	50 km	10 km	10 km
	LAI & SAI	10 km	50 km	1 km	10 km	50 km	10 km
	CLY	10 km	50 km	1 km	10 km	10 km	50 km
	Wind forcing	10 km					

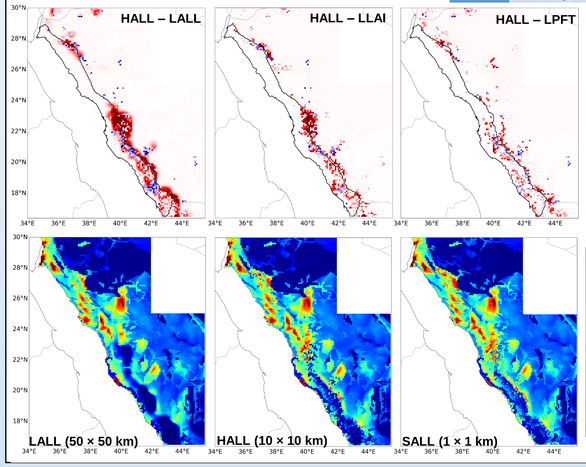

Second, we analyze the dust emission sensitivity to the resolution of the surface datasets without considering the contribution from each characteristic separately. We performed an additional **SALL** experiment, where the model was run with **1 × 1 km** grid and all the datasets taken with highest resolution possible. LALL, HALL and SALL served as basic simulations for comparisons with station observations with source function correction factors applied

Although the dust generation patterns are generally consistent, there are some substantial differences, most prominent between LALL and two other experiments. There are much more dust emitting areas in HALL and SALL simulations compared to LALL, especially in the southern region. SALL simulation is slightly more detailed along the transition zone (between plain and mountains) than HALL. Still, the difference between SALL and HALL is relatively small.

Models & methods

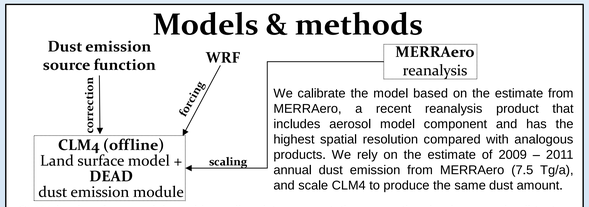

We calibrate the model based on the estimate from MERRAero, a recent reanalysis product that includes aerosol model component and has the highest spatial resolution compared with analogous products. We rely on the estimate of 2009 – 2011 annual dust emission from MERRAero (7.5 Tg/a), and scale CLM4 to produce the same dust amount.

CLM4 land surface model provides soil moisture, vegetation properties, land use, and soil texture to drive the DEAD module. CLM4 runs in offline mode, and is forced by meteorological fields provided by WRF. In the offline mode, CLM4 can be run at a finer spatial resolution than the driving meteorological model to account for high heterogeneity of land surface. Total dust emission flux to the atmosphere is calculated with the formula:

$$F = TSf_m \alpha Q_s$$

- f_m parameter is a grid cell fraction of soils suitable for dust mobilization, that depends on land fraction of bare soil, the plant function type (**PFT**), leaf area index (**LAI**), stem area index (**SAI**), and top soil layer water content;
- T is the tuning constant set to match MERRAero estimate;
- S is dust erodibility, set to 1 in default configuration or defined with **source function**;
- α is a sandblasting mass efficiency set by the mass fraction of clay particles (**CLY dataset**);
- Q_s parameter is the total horizontally saltating mass flux proportional to the third power of wind velocity when it exceeds threshold value.

Dust emission source functions

We use four types of dust emission source functions. Topographic source function is calculated following (Ginoux et al., 2001). Geomorphic source function was described by (Zender et al., 2003). MODIS and SEVIRI statistical source functions are based on AOD measurements from corresponding satellite instruments (Ginoux et al., 2010).

The MODIS instrument makes measurements twice a day; SEVIRI instrument is located on the geostationary satellite and provides measurements every 15 minutes

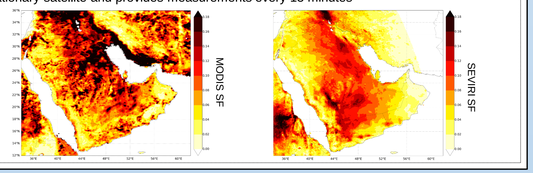

Results

- We present the results based on **1-km SALL simulation and SEVIRI source function**, that have the best skill (0.85) when compared with station observations.
- The spatial pattern of total dust emission is highly variable alongside the coastal area. The impact of high-resolution vegetation datasets is evident in the southern part, where the vegetation cover is dense. The dust generation pattern reasonably agrees with reanalysis, complementing it with high-resolution details.
- In the northern part of the coastal plain, dust emission reaches maximum in winter and spring, whereas in the south it is found in summer. This pattern is consistent with the seasonality of wind forcing.
- Dust emission hot spots are defined as areas where generated dust amount and emission frequency are two times higher, and dust event intensity is 1.5 time higher than domain-averaged values. The hotspots are located not right by the coastal areas, but rather near the western hillsides of Hejaz Mountains, in the dry riverbeds ("wadis") where the alluvial deposits are available.
- The annual dust emission from the 147000 km^2 coastal area scaled to match MERRAero reanalysis is 7.5 Tg. The total emission flux from the northern region is about 4.9 Tg/a, or 65% of the emissions from the entire coastal plain. This estimate highlights the importance of this dust source for supporting the nutrient balance of the oligotrophic northern part of the Red Sea.

Diurnal variability

Both total dust emission and frequency are peaked around late afternoon, at 12:00 – 14:00 UTC. The frequency of dust events during daily maximum is around 35% both in the north and in the south. Around 80% of airborne dust is generated between 07:00 – 16.00 UTC.

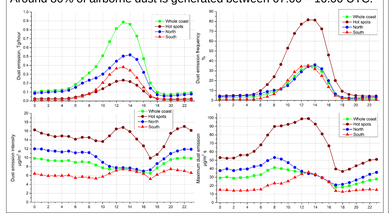

Seasonal variability

Different emission regimes in the northern and southern parts in caused by contrasting dust emission generation mechanisms. Winter – spring peak is not present in MERRAero due to the coarse resolution not allowing to simulate mesoscale circulation.

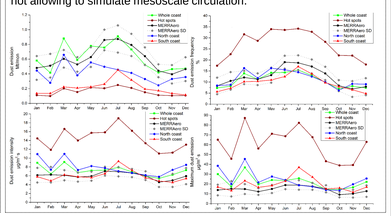

Total annual dust generation

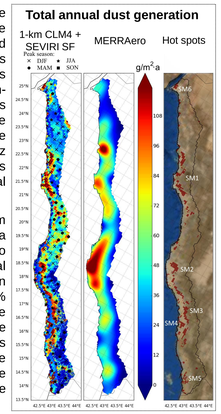

1-km CLM4 + SEVIRI SF

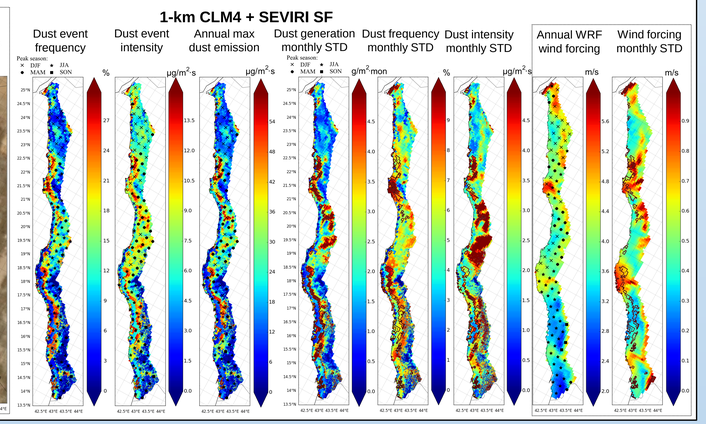

Conclusions

- The importance of using high-resolution input surface datasets was demonstrated. The resolution of vegetation datasets was shown to alter the total dust emissions up to 10%. Local changes in vegetated southern areas could be much stronger, with significant dust fluxes in high-resolution simulations from the zones where it was very weak when using coarse datasets.
- Encouraging results were obtained when using SEVIRI source function. Depending on model spatial resolution, the significant model skill varied from 0.68 to 0.85.
- The simulated dust emission patterns are in reasonable agreement with coarse-scale result from MERRAero global reanalysis, despite that reanalysis dust model uses different source function. The location of major dust hot spots mainly corresponds to so-called 'wadis' – lowland riverbeds that are usually considered as the source of alluvial material.
- The dust emission regime substantially differs for the northern and southern parts of the coastal plain. In the north, March is the peak month of dust activity, caused by strong, diurnally variable winds, while in the south annual maximum of dust emission occurs in July and is largely controlled by low erodibility threshold, soil moisture and source function correction factor. In reanalysis, only summer peak is present given that mesoscale winter wind circulation causing the March peak cannot be simulated.
- To assess the mineralogical composition of dust emission, we apply the dataset of soil mineralogy and texture (not shown here). 0.076 Tg of iron oxides and 0.006 Tg of phosphorus are emitted from the coastal plain annually. The northern dust hot spot areas in close proximity to the Sea that, in combination with the mesoscale jet winds and breezes could make these areas an essential source of nutrients for marine ecosystems.

Bibliography

1. Brindley, H. E., Ignatov, A. 2006. Retrieval of mineral aerosol optical depth and size information from Meteosat Second Generation SEVIRI solar reflectance bands. Remote Sensing of Environment, 102(3), 344-363.
2. Kalenderski, S., Stenchikov, G., Zhao, C., 2013. Modeling a typical winter-time dust event over the Arabian Peninsula and the Red Sea. Atmospheric Chemistry and Physics 13, 1999-2014.
3. Ginoux, P., Garbuzov, D., Hsu, N. C., 2010. Identification of anthropogenic and natural dust sources using Moderate Resolution Imaging Spectroradiometer (MODIS) Deep Blue level 2 data. Journal of Geophysical Research: Atmospheres, 115 (D5).
4. Ginoux, P., Chin, M., Tegen, I. et al., 2001. Sources and distributions of dust aerosols simulated with the GOCART model. Journal of Geophysical Research: Atmospheres, 106 (D17), 20255-20273.
5. Shao, Y., 2008. Physics and modelling of wind erosion. Springer Dordrecht, New York, NY.
6. Shi, M., Yang, Z. L., Stenchikov, G. L. et al., 2016. Quantifying the impacts of landscape heterogeneity and model resolution on dust emissions in the Arabian Peninsula. Environmental Modelling & Software, 78, 106-119.
7. Zender, C. S., Newman, D., Torres, O., 2003. Spatial heterogeneity in aeolian erodibility: Uniform, topographic, geomorphic, and hydrologic hypotheses. Journal of Geophysical Research: Atmospheres, 108 (D17).